PROCEEDINGS, Twenty-second Workshop on Geothermal Reservoir Engineering
Stanford University, Stanford, California, January 27-29. 1997
SGP-TR-155

FAULT ZONE ARCHITECTURE AND FLUID FLOW AN EXAMPLE FROM DIXIE VALLEY, NEVADA

Craig B. Forster, Jonathan S. Caine, Steven Schulz, Dennis L. Nielson

Energy & Geoscience Institute
Department of Civil and Environmental Engineering
The University of Utah
Salt Lake City, Utah

ABSTRACT

The permeability structure and stress state found within and near fault zones often determines rates and patterns of fluid flow in high-temperature geothermal systems. Unfortunately, insufficient subsurface information is available to adequately characterize the fluid flow properties of fault zones. In particular, we are unable to measure the in-situ variations in permeability, porosity, and storativity needed to assess their impact on geothermal production. We can, however, use outcrop analogs to aid in interpolating between wells and to provide a basis for extrapolating fluid flow properties from sparse wellbore data. A two-component fault zone model comprising damage zone and fault core provides a valuable framework for fault mapping. Detailed mapping of the geometry and distribution of each component, combined with measured fracture characteristics, yields the quantitative information needed to improve numerical models of fluid flow in fault-controlled geothermal systems. Integrated surface and subsurface data obtained at the Dixie Valley Geothermal Field is used to estimate input parameters for simulating fluid flow, heat transfer, and solute transport in this fault-controlled geothermal system.

INTRODUCTION

Production in many high-temperature geothermal systems is directly associated with high-permeability pathways for fluid flow provided by fault zones. Thus, an improved understanding of the magnitude and distribution of permeability within fault zones will aid in designing improved exploration and development strategies. Because previous studies suggest that the permeability structure of faults is largely controlled by their internal architecture [Forster and Evans, 1991; Forster et al., 1994; Goddard and Evans, 1995; Forster et al., in press; Caine et al., 19961we are attempting to better understand fault-related permeability structures in the Dixie Valley Geothermal Field by comparing observations made in outcrop to subsurface information. An important goal of this work is to develop quantitative predictive numerical models of fluid flow in fault-controlled geothermal systems. We adopt this approach because insufficient subsurface information are generally available to adequately characterize the permeability structure of fault zones. In particular, we are hindered by our inability to measure the in-situ variations in permeability, porosity, and storativity needed to assess their impact on production. Outcrop analogs are expected to aid interpolation between wells and provide a basis for extrapolating fluid flow properties from sparse wellbore data.

FAULT MODEL

Figure 1 shows a conceptual model for fault zones based on detailed outcrop mapping in diverse geological environments [Sibson, 1981; Chester and Logan, 1986; Parry and Bruhn, 1986; Forster and Evans, 1991; Goddard and Evans, 1995; Caine et al., 19961. This model provides a framework for determining spatial variability in fault zone architecture from field data and for incorporating physically-based geological information in mathematical models of fluid flow. Two primary fault zone components (fault core and damage zone) are shown in Figure 1 with the protolith stripped away. No scalar relationship is implied between the components, nor must each component be present in any given fault. The character, amount, and distribution of each Component controls the anisotropy and heterogeneity in permeability that, in turn, influences fluid flow within and near the fault [Forster and Evans, 1991; Caine et al., 19961.

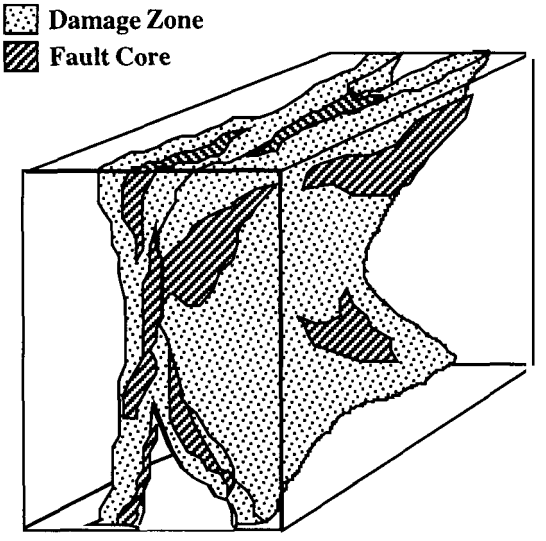

Figure 1: Conceptual model of fault zone architecture with protolith removed.

Note that the fluid flow properties of a fault zone may change through time, thus the diagram shown in Figure 1 represents only a single window in time. For example, the fault core may act as a conduit during deformation and as a barrier when open pore-space is filled by mineral precipitation following deformation. Temporal variations in the orientation and magnitude of tectonic stresses can also cause important changes in permeability structure. It is important to specify the stage of fault evolution when forming a conceptual model for a particular fault zone [Caine et al., 19961.

The range of possible fault zone architectures is illustrated in Figure 2. Each of the 4 end-member architectural styles is associated with a characteristic permeability structure. These include localized conduits, distributed conduits, localized barriers, and combined conduit-barriers [Caine et al., 19961.

The fault core is the structural, lithologic, and morphologic portion of a fault zone where most of the displacement takes place (Figure 1). Fault cores may include single slip surfaces, unconsolidated clay-rich gouge zones, brecciated and geochemically altered zones, or highly indurated, foliated ultracataclasite zones. Field-based observations suggest that variations in thickness, internal structure, and composition each play an important role in controlling fluid flow properties within a fault core. For example, the fault core may act as a relatively high-permeability conduit

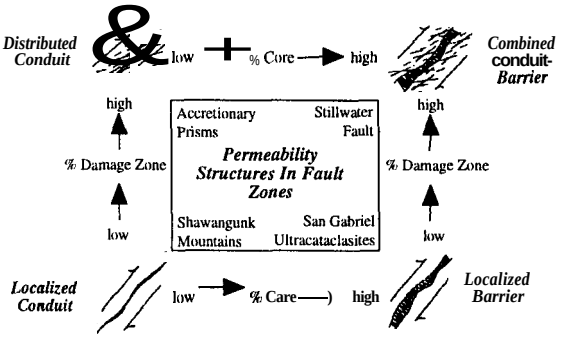

Figure **2:** Conceptual scheme for fault-related fluid flow [after Caine et al., 19961.

in geothermal systems. Exceptions to this are indicated where silicified pods of brecciated rock form low permeability zones or fluid flow baffles within the fault core. Grain-size reduction and/or mineral precipitation found in other, non-geothermal environments generally yield fault cores where reduced porosity and permeability yields baffles or barriers to fluid flow [e.g. Chester and Logan, 1986; Goddard and Evans, 1995].

A damaged zone (Figure 1) comprises the network of subsidiary structures that bound the fault core and typically enhance fault zone permeability relative to the undeformed protolith [Chester and Logan, 1986; Scholz and Anders, 1994; Goddard and Evans, 1995; Caine et al., 19961. Fault-related subsidiary structures in damage zones include small faults, veins, joints, cleavage, and folds that cause heterogeneity and anisotropy in the permeability structure and elastic properties of the fault zone [Forster et al., in press; Caine et al., 19961.

The fault core and damaged zones shown in Figure 1 are surrounded by relatively undeformed protolith. This is the country rock where fault-related permeability structures are absent and both fluid flow and elastic properties of the rock reflect those of the unfaulted host rock. Fault zone architecture may ultimately reflect the degree to which the processes of strain localization versus strain distribution compete as the fault zone cuts different rock types in the protolith [Caine et al., 19961.

The geometry and magnitude of permeability contrasts between the fault core and damage zone are primary controls on barrier-conduit systematics within the fault zone [Caine et al., 19961. In strike slip and

thrust fault environments fracture density in the fault core is often significantly less than that of the damage zone [Chester and Logan, 1986]. In these geologic regimes the permeability of the fault core may be dominated by the grain-scale permeability of the fault rocks while the damage zone permeability is dominated by the hydraulic properties of the fracture network [Caine et al., 19961. The converse may be more typical in the high temperature geothermal systems associated with faults found in extensional environments. Large fluid fluxes and elevated fluid temperatures found in such regimes may inhibit geochemical sealing processes within the fault core and produce highly permeable pathways within the core.

DIXIE VALLEY. NEVADA

Integrating the results of our outcrop studies with subsurface information collected at the Oxbow Geothermal Power Plant located within the Dixie Valley Geothermal Field (DVGF shown in Figure **3)** provides a basis for numerically simulating tracer tests within fault-controlled regions of the geothermal reservoir. Simulations of high-temperature fluid flow and tracer transport within a fault zone are currently underway [Rose et al., 19971.

Geologic Setting

The Dixie Valley Geothermal System is located on the western margin of Dixie Valley in central Nevada between the Stillwater and Clan Alpine ranges (Figure 3). Dixie Valley is an asymmetric basin [Anderson et al., 1983] bounded on the west by the Stillwater fault with a series of minor faults found along the eastern margin (Figure 3). At least 2000 m of fill are found along the western margin of the basin. Fill thickness decreases to the east. Structural relief due to both faulting and bending is about 2.9 km, and extension across the basin is about 20% [Okaya and Thompson,1985]. The Dixie Valley Geothermal Field is located near the northeast striking Stillwater fault (Figure 3). This fault is presently active, with the last major earthquake occurring in 1954 [Okaya and Thompson, 1985]. The fault dips 50" to 54" to the southeast [Okaya and Thompson, 1985; Wesnousky and Ojiambo, 19921.

A series of smaller, sub-parallel subsidiary faults found in the hanging wall of the Stillwater fault zone [Benoit, 1992; Wesnousky and Ojiambo, 19921 are not exposed at the surface, but can be seen in seismic profiles. Several wells drilled in the Dixie Valley Geothermal Field intersect and produce water from small subsidiary fault zones (displacements less than 400 m) found up to 1200 meters away from the Stillwater fault [Waibel, 1987; Benoit, 19921. We expect that our conceptual model of fault zone architecture likely applies equally well within both the main range bounding fault and within each of the

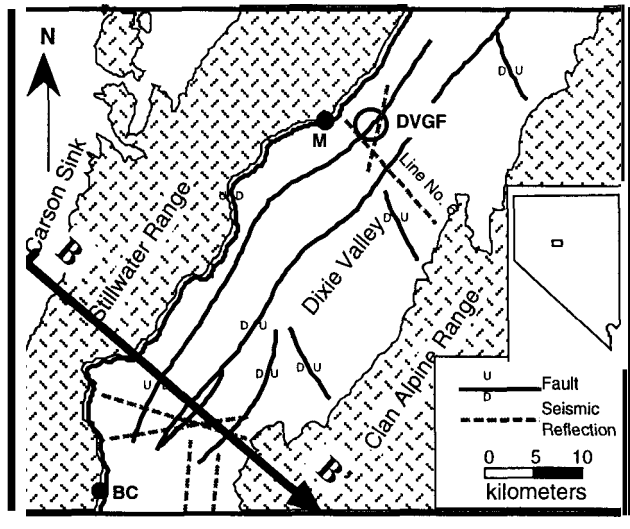

Figure **3:** Location map showing the relationship between mapped fault exposures (Mirrors [M] and Box Canyon [BC] localities), primary fault zones, seismic reflection lines, the Dixie Valley Geothermal Field (DVGF) and section line

small fault splays found in the hanging wall (Figure 4).

Fluid Flow Regime

Generalized patterns of subsurface fluid flow within the Dixie Valley groundwater/hydrothermal system are shown in Figure 6. Because Dixie Valley is a topographically closed basin, it seems reasonable to assume that all water entering the system is derived from precipitation on the surrounding mountain ranges. After circulating through the system water is likely discharged from the basin through evapotranspiration at the valley floor (at the Humboldt Salt Marsh). Although inter-basin transfer of groundwater may also occur, this process likely accounts for only a small portion of the total water budget for Dixie Valley.

Patterns and rates of fluid flow are influenced by the surface topography, geologically-controlled permeability structures, and the underlying heat flow regime. For example, schematic fluid flow patterns shown in Figure 5 suggest that meteoric water may penetrate deeply into the rocks of the Stillwater and Clan Alpine Mountains. Hot springs are often located where zones of enhanced permeability outcrop in groundwater discharge areas. For example, one set of hot springs shown in Figure 5 are found in the low-elevation groundwater discharge area associated with the Humboldt Salt Marsh. These springs are supplied by upflow along both the main range-bounding fault and one or more fault splays located basinward of the main fault. Moving away from the primary discharge area reduces the likelihood for hot springs because the water table lies at increasingly greater depth below the ground surface. Thus, the absence of hot springs near the Dixie Valley geothermal system suggests that hot water likely joins the shallow groundwater system below the ground surface before moving south to discharge in the Humboldt Salt Marsh.

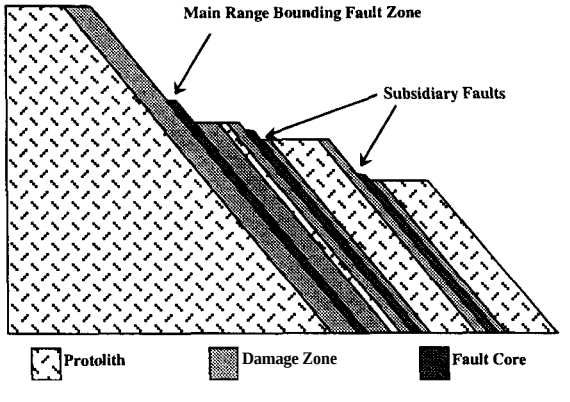

Figure 4: Conceptual model of fault-related structures in the Dixie Valley Geothermal Field.

The permeability structure of a fault zone plays an important role in controlling hydrothermal circulation and the development of hot springs. If the main range bounding fault shown in Figure 5 comprises a permeability barrier then groundwater circulation from the Stillwater Range to the basin would be inhibited and most hot springs might be found near the mountain front. Conversely, if the main range bounding fault comprises only a high permeability conduit then groundwater flowing through the mountain range will be more easily transferred to the adjacent basin and hot springs may be located further away from the mountain front.

Forster and Smith (1989) and Forster and Evans (1991) simulated coupled fluid flow and heat transfer in vertical sections containing simple fault-related permeability structures. Their results suggest that simulations performed within the vertical section of Figure 5 would yield a range of different thermal regimes, depending upon the permeability structure of the fault zones. Before these simulations can be performed, however, it has been necessary to establish geologically plausible permeability structures for the faults found in Dixie Valley. The following sections outline how we are using outcrop mapping of exhumed faults to improve our understanding of the permeability structure of fault zones.

Fault Zone Components Observed in Outcrop

Outcrop studies in Dixie Valley, Nevada (Forster et al., in press) have focused on detailed mapping of fracture networks found at two locations (Box Canyon and Mirrors localities) within the footwall of the main range bounding faults (Figure 3). The Mirrors site is close to the Dixie Valley Geothermal Field (Figure 3). These data have helped to revise our conceptual model of fault zone architecture (Figure 1) and yield constraints for ongoing efforts to simulate fluid flow within and near a fault zone. Contacts between fault core, damage zone, and protolith were mapped within a region extending over tens of square meters. Fracture data are tied together over several

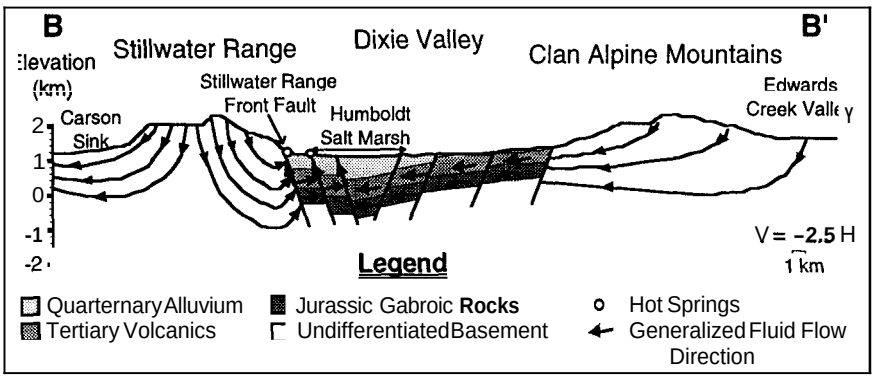

Figure 5: Schematic cross section and topographic profile from the Carson Sink through Dixie Valley to the Edwards Creek Valley (modified from Koenig et al., 1976) with inferred patterns of fluid flow. Section location is shown in Figure 3.

scales by centimeter-scale petrographic fracture analyses, meter-scale outcrop fracture analyses, and tens to hundreds of meters-scale fracture analyses using field mapping and low-elevation aerial photographs. In spite of the complicated fracture network found in this large fault zone, distinct kinematically-related fracture sets can be identified that likely have distinct permeability characteristics.

Protolith exposed at the Mirrors locality (Figure 3) is altered, fine to medium grained granodiorite [Forster et al., in press]. Alteration assemblages found in veins that are kinematically compatible with the master fault zone suggest that hydrothermal alteration within the fault zone was assisted by fluid flow through fracture networks open during faulting. Permeability testing of small (1-inch to 2-inch diameter) core plugs under a range of confining pressures suggests that the in-situ matrix permeability of the protolith is likely less than 10^{-18} m^2 (less than 10^{-3} md) [Forster et al., in press].

Damage zone rocks are also exposed in footwall rocks at the Mirrors locality. A gradational contact between the damage zone and protolith is marked by a decrease in fracture intensity when moving from damage zone to protolith. Damage zone thickness varies from 50 to 150 meters. Although the lack of hanging wall information complicates our effort to infer fault zone architecture within the hanging wall rocks of the nearby geothermal system, the fracture networks mapped within the damage zone provide direct insight into the permeability heterogeneity and anisotropy that control subsurface fluid flow. Permeability testing suggests an in-situ matrix permeability for the damage zone that is less than 10^{-18} m^2 (less than 10^{-3} md) [Forster et al., in press]. This is similar to the results obtained for the protolith samples.

The highly fractured and veined granodiorite protolith found in the damaged zone contains extensional, shear, and cross fractures. Rough-walled, extension fractures are strike-parallel with the master fault but the fractures dip more steeply than the fault. These fractures often contain precipitated mineral fillings. Shear fractures containing small faults with less than 5 cm of offset are also strike parallel with the master fault but the fractures dip less steeply than the fault. Some shear fractures have polished and striated surfaces, and when filled, often contain porphyroclasts. Two moderately dipping sets of cross fractures are identified that are not strike parallel with the master fault.

The fault core at the Mirrors locality comprises a 15 to 40 meter wide zone with large curviplanar, striated, and polished slip surfaces up to 25 m^2 in area. These surfaces cut, and in some locations bound, a tectonically-derived quartz-breccia zone that marks the silicified core of the range bounding fault. The breccia zone is typified by pods of highly silicified breccia enveloped by less silicified, fine grained, and pervasively veined cataclastic rocks. Breccia pods range from 3 to 30 meters in length and from 2 to 6 meters in thickness. Sample and outcrop observations suggest that the breccia zones may represent localized sites of tectonically-driven hydrothermal implosion brecciation [Sibson, 1981] that originally produced localized zones of high permeability that are now silicified. Permeability testing suggests that the in-situ matrix permeability of the core rocks is less than

either the protolith or damage zone with values less than 10^{-19} m^2 (less than 10^{-4} md) [Forster et al., in press]. Prior to silicification, however, unfilled fractures would likely have yielded much higher permeabilities [Lutz, 1995].

Although the fault core is fractured and contains veins, fracture intensities are typically lower than those of the adjacent damage zone while fracture orientations in the core are similar to those identified in the damage zone) [Forster et al., in press]. Fracture intensity varies within the fault core with minimal fracturing found in the highly silicified breccia pods.

Subsurface Data

The results of a tracer test begun in 1996 [Rose et al., 1997] provide direct insight into the contemporary fluid flow properties of a splay of the range bounding fault (Figure 5). Initial results suggest that the peak breakthrough concentration of a tracer injected at one well within the fault splay is expected to travel approximately 1.7 km in 270 days [Rose et al., 19971. Preliminary modeling results suggest that the bulk permeability of the fault zone must exceed 10^{-14} m^2 (10 md) and is likely on the order of 10^{-12} m^2 (1,000 md). We infer that the overall structure resembles a scaled down version of the architecture mapped in outcrop within the footwall of the nearby range bounding fault.

Each of the fracture sets identified in the Mirrors outcrop are also found in televiewer logs of the primary producing interval (about 2.5 km deep) located in Well 73-B7 that penetrates a fault splay in the vicinity of the tracer test [Barton et al., 19971. Analysis of spinner and pressure logs [Barton et al., 1997] suggests that the most permeable fracture sets are associated with the extension and shear fractures mapped in outcrop. Permeability values computed from the spinner and pressure logs are on the order of 2×10^{-11} to 5×10^{-11} m^2 20,000 to 50,000 md) [Barton et at., 19971. After measuring fracture orientations, fracture intensities, and apparent fracture apertures in the primary producing zone of Well 73B-7 (between depths of 2440 to 2640 meters), Barton et al. [1997] found that the smallest fracture intensities and largest fracture apertures are located in the bottom 50 m of the measured interval. Insufficient data are available, however, to establish whether this 50 m section represents the fault core or the damaged zone.

MODELING FLUID FLOW WITHIN A FAULT ZONE

Our strategy for modeling fluid flow within a fault zone involves using an architectural model constrained by outcrop data as a framework for establishing permeability heterogeneity and anisotropy. Because geothermal systems are typically developed in low-permeability rocks where fracture permeability dominates, equivalent porous media permeabilities must be estimated for each fault component by upscaling and averaging the fluid flow properties of fracture networks associated with each component. A deterministic approach is currently being used to create the plausible permeability structures needed to simulate fluid flow and solute transport within a fault.

To date most of our fracture network modeling [Forster et al., in press] has employed a relatively simple method outlined by Oda et al. [1987]. Recently, however, we have begun to use Fracman [Dershowitz et al., 1995] to develop more sophisticated models of 3-D fracture networks and we are exploring other emerging methods [e.g., Koebbe and Hestir, 1992; Mauldon et al., 1993; Doughty et al., 19941. Unfortunately, data required as input to fracture network models is not often collected in standard structural mapping activities. For example, quantitative estimates of fracture length, fracture density, orientation, aperture, termination style, aspect ratio of shapes of fracture planes, fracture roughness, and relative proportions of each fracture set are required. Even when some of these data have been collected by other workers, the data collection points have not been tied into a coherent fault zone model such as the conceptual model outlined above. Thus, we find that we must augment previously collected data with new data in order to produce suitable input for a component-based fault zone model.

Preliminary simulations of fluid flow, heat transfer, and solute transport within a splay of the range bounding fault zone are underway using TOUGH2 [Pruess, 19911. As a first step we have adopted a simple rectangular fault zone geometry with homogeneous and isotropic permeability within a patch of the fault splay [Rose et al., 1997]. The initial set of boundary conditions are set by assuming the impact of regional, topographically driven fluid flow is minimal. A suite of injection and production wells involved in the 1996 tracer test [Rose et al 19971 are

included within the model domain. Iinitial results suggest that permeabilities estimated by Barton et al. [1997] in the production zone of Well 73-B7 are consistent with the values needed to support the observed tracer history. A bulk permeability in excess of 10^{-12} m^2 (1,000 md) is required to model the damage zonelcore composite.

CONCLUSIONS

Outcrop assessment of faults in general, and the Stillwater fault zone in particular, provide insight that helps to develop improved numerical models of fluid flow within the fault-controlled Dixie Valley Geothermal Field. Although the hanging wall rocks found in the primary producing zones are not exposed in outcrop, the footwall exposures do provide important insight into fault zone architecture and the character of dominant fracture networks. For example, footwall exposures yield insight into the fracture systems that contribute to fluid flow (e.g., fracture trace lengths, orientations, fracture intensities, and variations in fracturing as a function of fault zone component type). Initial fluid flow modeling using a porous media equivalent to the fracture networks that control flow suggest that bulk permeabilities within the damage zonelcore composite must exceed 10^{-12} m^2 (1,000 md). This inference is consistent with subsurface information collected by Barton et al. [1997]. Future modeling studies to be performed both at the fault zone and basin scales will be constrained by estimating heterogeneity and anisotropy within the fault zone using outcrop data to obtain a more complete set of fracture network models.

ACKNOWLEDGEMENTS

This report was compiled using funding from U. S. Department of Energy contract # DE-AC07-95ID13274. Forster was also funded by USGS NEHRP Grant # 1434-93-G-2280.

REFERENCES

Anderson, R. E., Zoback, M. L. and Thompson, G. A., 1983, Implications of selected subsurface data on the structural form and evolution of some basins in the northern Basin and Range province, Nevada and Utah: Geological Society of America Bulletin, v. 94, p. 1055-1072.

Barton, C.A., Hickman, S., Morin, R., Zoback, M.D., Finkbeiner, T., Sass, J., and D. Benoit, 1997, Fracture permeability and its relationship to in-situ stress in the Dixie Valley, Nevada, geothermal reservoir: Twenty-second Annual Workshop on Geothermal Reservoir Engineering, Stanford, CA, Jan. 27-29, 1997, this volume.

Benoit, D., 1992, A case history of injection through 1991 at Dixie Valley, Nevada: Geothermal Resources Council Transactions, v. 16, p. 611-620.

Caine, J.S., Evans, J.P., and C.B. Forster, 1996, Fault zone architecture and permeability structure: Geology, v. 24, pp. 1025-1028.

Chester, F. M. and Logan, J. M., 1986, Composite planar fabric of gouge from the Punchbowl Fault, California: Journal of Structural Geology, v. 9, p. 621-634.

Dershowitz, W., Lee, G., Geier, J., Foxfors, T., LaPointe, P., and A. Thomas, 1995, Fracman interactive discrete feature data analysis, geometric modeling and exploration simulation: Golder Associates, Seattle Washington.

Doughty, C., Long, J.C.S., Hestir, K., and S.M. Benson, 1994, Hydrologic characterization of heterogeneous geologic media with an inverse method based on iterated function systems: Water Resources Research, v. 30, p. 1721-1745.

Forster, C. B. and Evans, J. P., 1991, Hydrogeology of thrust faults and crystalline thrust sheets: results of combined field and modeling studies: Geophysical Research Letters, v. 18, p. 979-982.

Forster, C.B., and L. Smith, 1989, The influence of groundwater flow on thermal regimes in mountainous terrain: A model study, Journal of Geophysical Research, 94(B7), 9439-9451.

Forster, C.B., Bruhn, R.L., Fredrich, J., Caine, J.S., Seront, B., and T-f. Wong, (in press), Field and Laboratory Study of the Spatial and Temporal Variability in Hydromechanical Properties of an Active Normal Fault Zone, Dixie Valley, Nevada: U.S. Geological Survey, NEHRP, Final Technical Report.

Forster, C. B., Goddard, J. V., and Evans, J. P., 1994, Permeability structure of a thrust fault, in The Mechanical Involvement of Fluids in Faulting: extended abstracts of the U.S.G.S. 1994 Red-Book Conference: Open-File Report # 94-228, p. 216-223.

Goddard, J. V. and Evans, J. P., 1995, Chemical changes and fluid-rock interaction in faults of crystalline thrust sheets, northwestern Wyoming, U.S.A.: Journal of Structural Geology, v. 17, p. 533-547.

Koebbe, J.V., and K. Hestir, 1992, Inverse modeling using simulated annealing with homogenization: Proceedings of the IX International Conference on Computational Methods in Water Resources, June 9-12, 1995, p. 421-428.

Koenig, J.B., Greensfelder, R.W., and C.W. Klein, 1976, Geothermal potential of the Quest leasehold, Dixie Valley, Nevada: GeothermEx, Inc., Berkeley, CA.

Lutz, S.J., 1995, Mineralogic and petrographic analysis of outcrop samples from the Dixie Valley fault zone, Nevada: Unpublished internal report, Earth Sciences and Resources Institute at the University of Utah, 18 p.

Mauldon, A.D., Karasaki, K., Martel, S.J., Long, J.C.S., Landsfeld, M., and **A.** Mensch, 1993, An inverse technique for developing models for fluid flow in fracture systems using simulated annealing: Water Resources Research, v. 29, p. 775-3789.

Oda, M., Hatsuyama, Y., and Y. Onishi, 1987, Numerical experiments on permeability tensor and its application to jointed granite at the Stripa Mine, Sweden: J. Geophys. Res., v. 92, p. 8037-8048.

Okaya, D. A. and Thompson, G.A., 1985, Geometry of Cenozoic extentional faulting: Dixie Valley: Tectonics, v. 4, p. 107-125.

Parry, W. T. and Bruhn, R. L., 1986, Pore fluid and seismogenic characteristics of fault rock at depth on the Wasatch Fault, Utah: Journal of Geophysical Research, v. 91, p.730-744.

Pruess, K., 1991, TOUGH 2 - A general purpose numerical simulator for multiphase fluid and heat flow: Report LBL-29400, Lawrence Berkeley Laboratory, Berkeley, CA.

Rose, P.E., Apperson, K.D., Johnson, S.D., and M.C. Adams. 1997, Numerical simulation of a tracer test at Dixie Valley. Twenty-Second Annual Workshop on Geothermal Reservoir Engineering, Stanford, CA, Jan. 27-29, 1997, this volume.

Sibson, R. H., 1981, Fluid flow accompanying faulting: field evidence and models, in Simpson, D.W. and Richards, P.G., eds., Earthquake Precdiction-An International Review: Maurice Ewing Series 4, American Geophysical Union Monograph, p. 593-603

Waibel, A.F., 1987, An Overview of the geology and secondary mineralogy of the high temperature geothermal system in Dixie Valley, Nevada: Geothermal Resources Council, Transactions, v. 11, p. 479-486.

Wesnousky, S.G. and Ojiambo, B., 1992, Reconnaissance of geological and geophysical data available to understand tectonic controls on the occurrence of geothermal energy in Dixie Valley, Nevada and elswhere in the Basin and Range: Unpublished Report by the Center fo Neotectonic Studies, University of Nevada, Reno, NV.